View metadata, citation and similar papers at core.ac.uk
brought to you by CORE
provided by Elsevier - Publisher Connector

Neuron, Vol. 40, 139–150, September 25, 2003, Copyright ©2003 by Cell Press

Hypocretin (Orexin) Induces Calcium Transients in Single Spines Postsynaptic to Identified Thalamocortical Boutons in Prefrontal Slice

Evelyn K. Lambe* and George K. Aghajanian
Departments of Psychiatry and Pharmacology
Yale School of Medicine
New Haven, Connecticut 06519

Summary

In vivo, thalamocortical axons are susceptible to the generation of terminal spikes which antidromically promote bursting in the thalamus. Although neurotransmitters could elicit such ectopic action potentials at thalamocortical boutons, this hypothesis has never been confirmed. Prefrontal cortex is the cortical area most implicated in arousal and is innervated by thalamic neurons that are unusual since they burst rhythmically during waking. We show that a neurotransmitter critical for alertness, hypocretin (orexin), directly excites prefrontal thalamocortical synapses in acute slice. This TTX-sensitive activation of thalamic axons was demonstrated electrophysiologically and by two-photon sampling of calcium transients at single spines in apposition to thalamic boutons anterogradely labeled in vivo. Spines receiving these long-range projections constituted a unique population in terms of the presynaptic excitatory action of hypocretin. By this mechanism, the hypocretin projection to prefrontal cortex may play a larger role in prefrontal or "executive" aspects of alertness and attention than previously anticipated.

Introduction

Hypocretin (orexin) is essential for normal wakefulness (Sutcliffe and de Lecea, 2002), and it is almost undetectable in most patients with narcolepsy (Peyron et al., 2000; Ripley et al., 2001; Thannickal et al., 2000). The narcoleptic phenotype is seen in mice lacking the precursor preprohypocretin (Chemelli et al., 1999) and in dogs lacking hypocretin receptor 2 (Lin et al., 1999). Levels of awareness and sleep involve interactions between thalamus and cortex (McCormick and Bal, 1997); the "nonspecific" midline and intralaminar thalamic nuclei appear to be particularly important in this regard (Groenewegen and Berendse, 1994; Jones, 2001; Steriade et al., 1993). Neurons from these nuclei project to prefrontal cortex, especially anterior cingulate (Berendse and Groenewegen, 1991; Marini et al., 1996), and promote cortical activation (Groenewegen and Berendse, 1994). Hypocretin has recently been shown to depolarize nonspecific thalamic neurons through the hypocretin receptor 2 (Bayer et al., 2002). If these hypocretin receptors were also present in the axonal compartment of thalamic cells, thalamocortical boutons would be directly depolarized by hypocretin released in prefrontal cortex. This phenomenon is of interest since thalamocortical terminals are susceptible to the generation of terminal spikes (Gutnick and Prince, 1972; Pinault and Pumain, 1989) that promote synchronized bursting of thalamic neurons (McCormick and Contreras, 2001; Pinault, 1995). Intralaminar thalamic neurons are unusual in that they exhibit such rhythmic bursting in the awake animal (Steriade et al., 1993).

Prefrontal cortex and, in particular, anterior cingulate activity correlates with level of arousal (Hofle et al., 1997; Paus et al., 1998; Yamasaki et al., 2002) and plays a critical role in attention. Although the older literature is conflicting with regard to the nature of cognitive deficits in narcolepsy, a recent study which controlled for alertness has emphasized that specifically "executive" or prefrontal aspects of attention are affected (Rieger et al., 2003). Another study showed abnormal frontal physiology in narcoleptics during preattentive and attentive tasks (Naumann et al., 2001). Although prefrontal cortex is innervated by hypocretin-containing axons (Fadel and Deutch, 2002; Peyron et al., 1998) and appears to receive projections from a unique population of hypocretin neurons with minimal collaterals (Fadel et al., 2002), the cellular effects of hypocretin have not yet been examined in prefrontal cortex. We use a triple-labeling technique together with two-photon imaging to show that hypocretin induces calcium transients selectively in single spines postsynaptic to identified thalamocortical boutons. The finding that hypocretin can excite the final synapse in the ascending arousal pathway, together with the unusual properties of thalamic terminals, suggests that hypocretin within prefrontal cortex could have profound effects in vivo on the thalamocortical interactions that underlie arousal and attention.

Results

Hypocretin Triggers Release of Glutamate onto Layer V Pyramidal Neurons in Prefrontal Cortical Slice

Hypocretin receptor 2 stimulation has recently been shown to excite nonspecific thalamic neurons (Bayer et al., 2002) that are known to project to prefrontal cortex (Berendse and Groenewegen, 1991). If, as postulated, this receptor is trafficked to thalamic axons, then thalamocortical boutons would also be directly depolarized. These terminals have previously been shown to be susceptible to the generation of terminal or "ectopic" spikes (Gutnick and Prince, 1972; Pinault and Pumain, 1989). In prefrontal slice, hypocretin-2 peptide elicited a dramatic increase in spontaneous postsynaptic currents in layer V pyramidal neurons without directly depolarizing the cells. As illustrated in Figures 1A and 1B, these postsynaptic currents could be blocked with a glutamate receptor antagonist (3 μM LY 293558, 3 min; $n = 5$ neurons at -70 mV) revealing them to be spontaneous excitatory postsynaptic currents (sEPSCs). Consistent with a depolarizing mechanism, hypocretin-induced sEPSCs were suppressed by TTX ($n = 5$ neurons; 1 μM TTX, 3 min), as illustrated in Figure 1C. Note that in the presence of TTX,

*Correspondence: evelyn.lambe@yale.edu

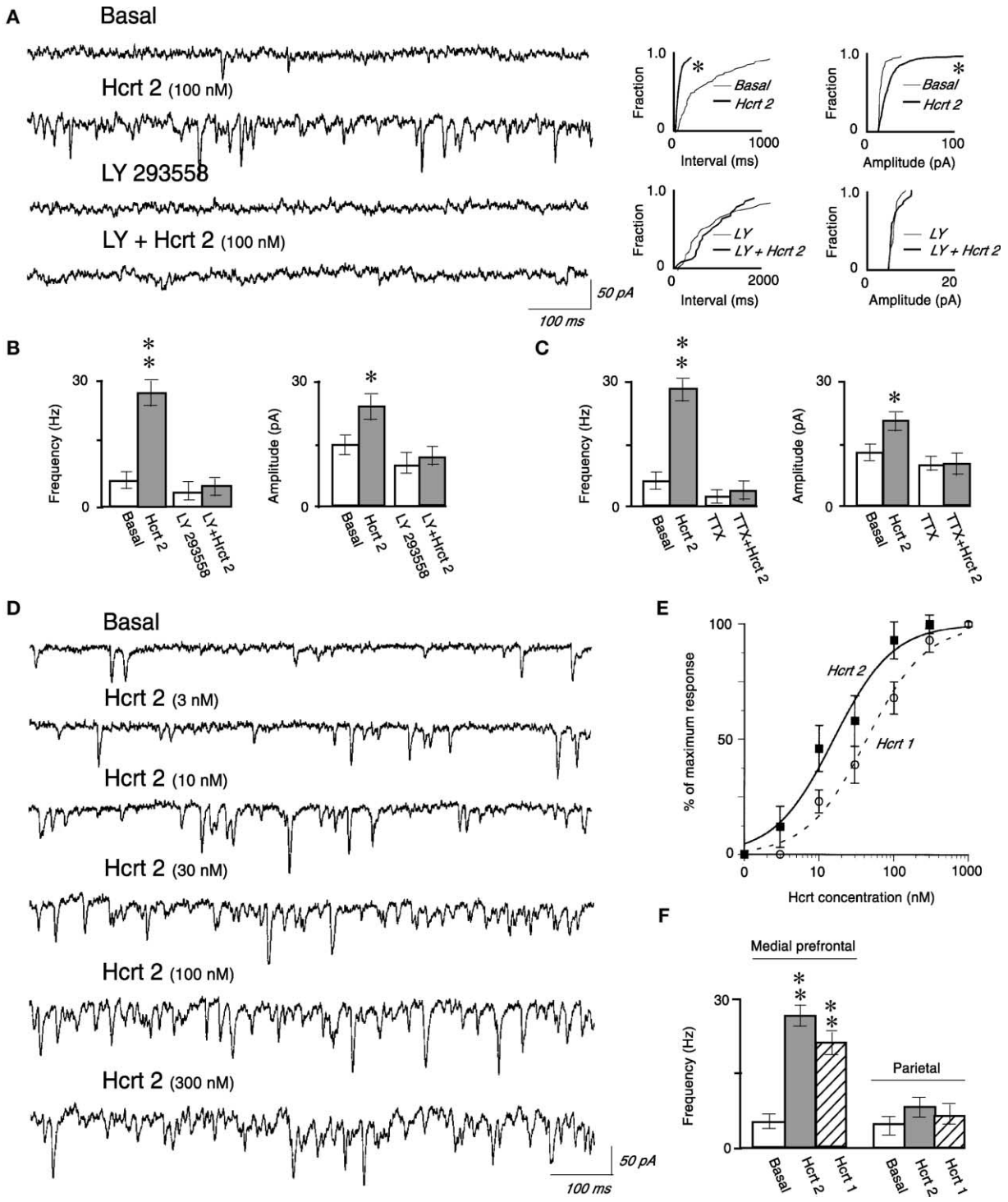

Figure 1. Hypocretin-2 Triggers Glutamate Release onto Layer V Pyramidal Neurons in Anterior Cingulate Slice

(A) Sweeps in voltage clamp from one neuron show a marked increase in spontaneous postsynaptic currents (sPSCs) induced by hypocretin-2 peptide. At −70 mV holding potential, application of the AMPA/KA glutamate receptor antagonist LY293558 (3 μM, 3 min) virtually eliminates the increase in sPSCs with hypocretin-2, indicating their identity as excitatory sPSCs (sEPSCs). To right, illustrative cumulative fraction curves for interevent interval and amplitude are shown for sEPSCs in this cell induced by 100 nM hypocretin-2 under baseline conditions (*$p < 0.001$; Kolmogorov-Smirnov test) and the lack of sEPSCs induced in the presence of LY293558.

(B) Mean ± SEM for increase in frequency and amplitude of sEPSCs by 100 nM hypocretin-2 and the loss of this increase in the presence of LY293558 ($n = 6$ neurons; **$p < 0.001$; *$p < 0.01$).

(C) The glutamate release triggered by hypocretin-2 is sensitive to the fast sodium channel blocker TTX (1 μM, 3 min; $n = 5$ neurons; **$p < 0.001$; *$p < 0.01$).

(D) Sweeps in voltage clamp from one neuron show basal EPSCs and those induced by bath application of hypocretin-2 in different concentra-

hypocretin did not increase miniature EPSC amplitude, arguing against a postsynaptic action of hypocretin.

Dose response was assessed in a subgroup of neurons (n = 5; all concentrations tested in each neuron) using a broad range of hypocretin-2 concentrations (1 nM to 300 nM). An example is shown in Figure 1D and a dose response curve in Figure 1E. The high sensitivity (EC_{50} = 16 nM) is congruent with that previously shown for the sensitivity of the somatodendritic hypocretin receptor 2 to the hypocretin-2 peptide in the thalamus (Bayer et al., 2002). Since the hypocretin-1 (orexin A) peptide also has high affinity for the hypocretin receptor 2 in addition to the hypocretin receptor 1 (Sakurai et al., 1998), we measured dose response for this peptide in a subgroup of neurons (n = 4 neurons; all concentrations tested in each neuron) and found sensitivity (EC_{50} = 40 nM) congruent with that shown for the sensitivity of the somatodendritic hypocretin receptor 2 to the hypocretin-1 peptide in the thalamus (Bayer et al., 2002).

In contrast with neurons recorded in medial prefrontal cortex, layer V pyramidal neurons in parietal cortex in the same slice—a region innervated sparsely by the midline and intralaminar thalamic nuclei (Berendse and Groenewegen, 1991)—showed only a minimal increase in sEPSCs in response to bath application of hypocretin-2 peptide or the hypocretin-1 peptide (100 nM, n = 6 neurons), as illustrated in Figure 1F.

For all further experiments, we used only the hypocretin-2 peptide because of its selectivity in activating hypocretin receptor 2. Hence, "hypocretin" or "hcrt" refers to hypocretin-2 peptide in all subsequent discussion of results and figures.

Hypocretin Triggers Repeated Postsynaptic Calcium Transients in a Subset of Spines

Two-photon imaging was used to identify synapses at which hypocretin induced glutamate release. Previously, it has been shown that subthreshold electrically evoked synaptic glutamate release leads to NMDA channel-dependent postsynaptic calcium transients in dendritic spines (Kovalchuk et al., 2000; Mainen et al., 1999; Oertner et al., 2002; Yuste and Denk, 1995). However, detecting hypocretin-induced postsynaptic calcium transients is more complicated because the location and timing of these events are not synchronized to a stimulus nor localized to spines near a stimulating electrode. Therefore, we adopted a sampling procedure.

We filled layer V pyramidal neurons (n = 5 neurons, each in a different slice) with a combination of Oregon green BAPTA-1 (100–200 μM) and Alexa 594 (10–20 μM) through the patch pipette. As illustrated in Figure 2A, under baseline conditions, this combination of dyes gave an orange appearance to the neuron in the merged image. When spiking opened voltage-gated calcium channels, the neuron turned yellow in appearance due to the selective increase in the intensity of Oregon Green BAPTA-1. To maximize the chance of detecting postsynaptic calcium transients, neurons were voltage clamped at −60 mV in 0.25–0.5 mM Mg^{2+} ACSF to enhance detection of NMDA-mediated synaptic transients. Spontaneous EPSCs were measured continuously during scanning. Regions of dendrite with several spines in focus were selected for imaging. To minimize risk of photobleaching and phototoxicity, scans were taken at intervals of 2 or 3 s during baseline, bath application of hypocretin, and washout. To assess calcium influx through voltage-gated calcium channels during spiking, a depolarization-induced burst of spikes was triggered late in the washout period or, occasionally, in a separate scan of this region. A burst was used because the regions sampled included dendrites in layer I, which showed minimal change to a single spike as expected from previous work (Helmchen et al., 1999).

Only a small subset of spines showed significant changes during application and washout of hypocretin, while a burst of action potentials increased the G/R ratio in all spines. Spines showing a change with hypocretin at least four standard deviations from baseline ($Z \geq 4$) were classed as "responders." Above this Z score, a dramatic change is observable to the naked eye; see, for example, the spine in the inset of Figure 2B. All responding spines showed repeated, large calcium transients during the time period that hypocretin-induced sEPSCs were detected electrophysiologically (voltage sweeps shown beneath two-photon images in Figure 2B). Due to the periodic nature of our sampling parameters, these calcium transients give only a minimum limit for the number of postsynaptic events at each spine.

Responding spines (n = 7, from six regions of dendrite) were all found on branches of the apical dendrite, including branches in the apical tuft (past the main bifurcation), as described in Table 1. The graph in Figure 2C compares peak Z scores during spikes and hypocretin for spines from the six regions in which a responder was detected (responders, n = 7; nonresponders, n = 22). While responding spines showed large peaks in G/R ratio during hypocretin-induced sEPSCs, after these peaks were excluded from the analysis, the average G/R ratio did not change significantly for either group (nonresponders: basal, 0.37 ± 0.02; hypocretin, 0.38 ± 0.04; responders: basal, 0.37 ± 0.03; hypocretin, 0.38 ± 0.04). The lack of change in the average G/R ratio in responders suggests that calcium levels, while they may have transiently increased, did not remain elevated.

Large calcium transients at responding spines were observed again upon a repeat application of hypocretin (n = 5). Consistent with the electrophysiology, TTX (1 μM) eliminated calcium transients at responding spines as well as almost all hypocretin-induced sEPSCs (n = 2; data not shown). By contrast, ACSF containing higher magnesium to block NMDA channels (2 mM Mg^{2+}, 5 min)

tions between 3 and 300 nM (10–25 min washout before subsequent application).

(E) Dose response curves from 20 1 s sweeps from the peak response period show increase in sEPSC frequency as a function of either hypocretin-2 (n = 5 neurons) or hypocretin-1 concentration (n = 4 neurons). All concentrations were tested in each neuron.

(F) The glutamate release triggered by either hypocretin-2 or hypocretin-1 (100 nM, 1 min) was much greater in medial prefrontal cortex (n = 4 neurons) than in parietal cortex (n = 6 neurons). "Hypocretin" or "Hcrt" refers to hypocretin-2 peptide in all subsequent experiments.

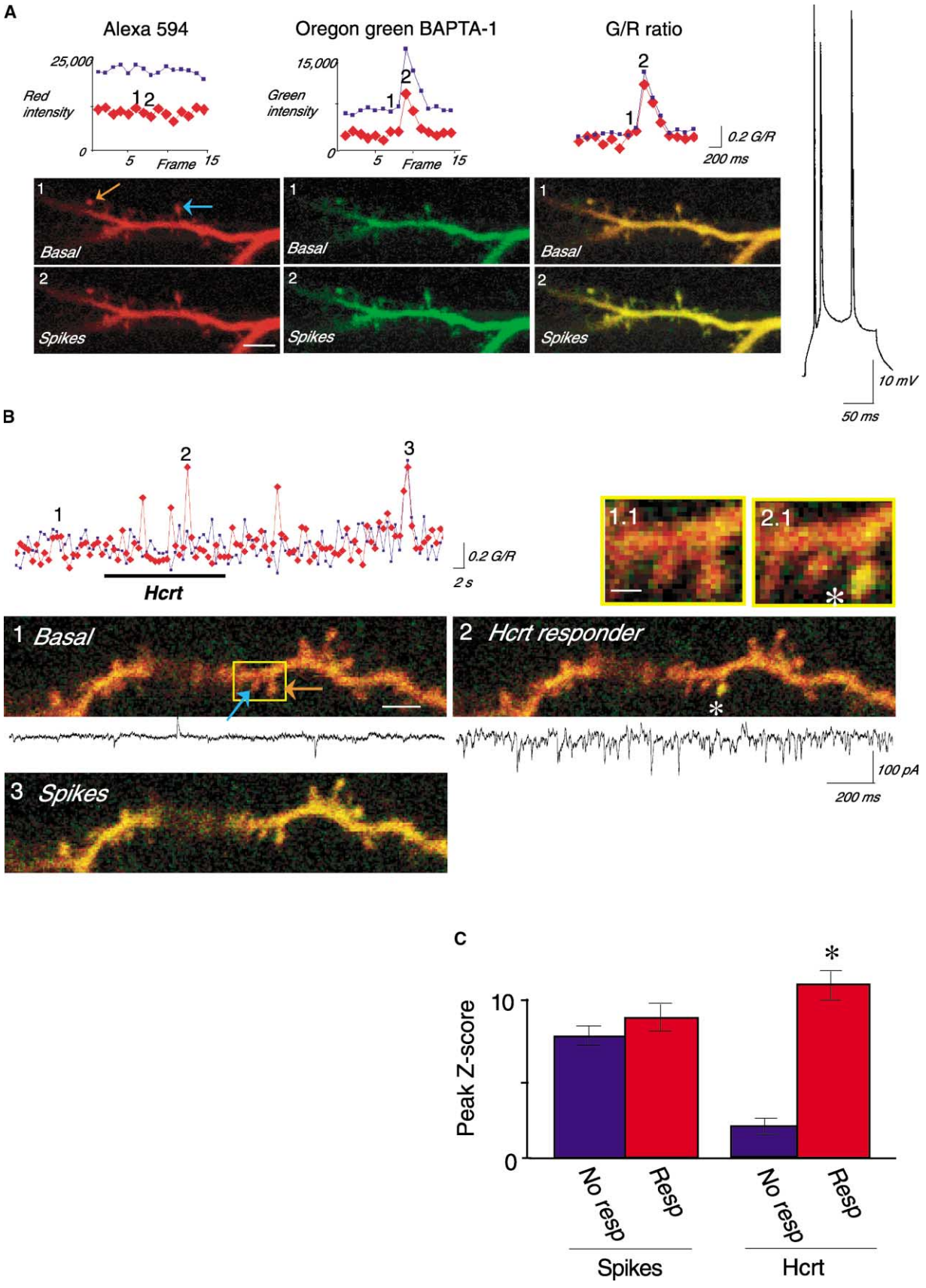
A
Alexa 594
Oregon green BAPTA-1
G/R ratio
25,000
Red intensity
15,000
Green intensity
Frame
0.2 G/R
200 ms
Basal
Spikes
10 mV
50 ms
B
Hcrt
0.2 G/R
2 s
1.1
2.1
1 Basal
2 Hcrt responder
3 Spikes
100 pA
200 ms
C
Peak Z-score
10
0
No resp
Resp
Spikes
Hcrt

Table 1. Dendritic Distribution of Spines that Respond to Hypocretin

Type of Dendrite	Regions Sampled	Responding Spines	Nonresponding Spines
Basal	4	0	16
Apical: main trunk	3	0	18
Apical: oblique	5	3	26
Apical: tuft	8	4	39
Total	20	7	99

reversibly attenuated calcium transients in response to hypocretin without blocking hypocretin-induced sEPSCs (n = 3; data not shown).

In the same neurons in which at least one region with a responding spine was detected, no responding spines were detected in an additional 14 regions of apical (n = 10) and basal dendrites (n = 4) scanned. These 14 regions contained 77 spines in focus that responded to spiking but not to hypocretin. In all regions scanned, 7/106 spines responded to hypocretin. All responding spines were on branches of the apical dendrites. While the above results showed that a small subset of spines exhibit calcium transients in response to hypocretin, it was not possible to determine by this approach whether these spines were differentiated from nonresponding spines by the presence of thalamocortical input.

Labeling Thalamocortical Projections

Although the apical dendritic location of the responding spines would be congruent with excitation of direct thalamic input, these findings do not identify which glutamatergic projections are excited by hypocretin. Further experiments were pursued to test our hypothesis that the increase in glutamatergic sEPSCs seen in layer V neurons resulted from direct stimulation by hypocretin of thalamic boutons terminating on these cells.

Projections from the midline and intralaminar thalamic nuclei to the anterior cingulate were labeled by electroporation with the anterograde tracer *Phaseolus vulgaris* conjugated with Alexa 488 (PHAL488) in vivo 2–4 days before recording. Figure 3A shows a two-photon image of thalamic neurons filled with PHAL488 in a coronal slice through the anterior thalamus. Figure 3B shows filled thalamocortical axons coursing through the white matter of the cingulum en route to prefrontal cortex in a horizontal slice. For further experiments, the usual acute coronal slices of prefrontal cortex were employed. Labeled axons, boutons, and terminals were found throughout cingulate cortex with a higher density of axons and boutons in layer V, as well as in superficial layers, including layer I, as expected from past anatomical labeling studies (Berendse and Groenewegen, 1991; Marini et al., 1996).

Calcium Transients Appear Selectively in Spines Receiving Thalamic Input

After filling layer V pyramidal neurons with Oregon green and Alexa 594 (n = 4 neurons in 4 slices), we found scattered appositions in the *x-y* plane between labeled boutons and dendritic spines. As shown in Figure 4, the combination of Oregon green and Alexa 594 rendered the pyramidal neurons orange in appearance and hence readily distinguishable in a merged image from the purely green PHAL488-labeled boutons (e.g., appositions shown in inset figures; Figures 4A and 4B). Just as only a fraction of spines responded to hypocretin in our previous experiments, apparent appositions between labeled boutons and spines were infrequent. Although a systematic survey was not attempted, the occurrence of appositions appeared greatest on branches of the apical dendrite, particularly beyond the main branch point, similar to the distribution found previously for responding spines. As the occurrence of appositions does not prove functional synaptic junctions, we studied the actions of hypocretin at spines with apparent appositions, using calcium imaging techniques as described above.

Of seven regions imaged containing apparent appositions in the *x-y* plane between an orange spine head and a green PHAL488-labeled bouton, there were eight spines that appeared to abut seven PHAL488-labeled boutons (see Figure 4B for an example of two spines appearing to touch the same bouton). Hypocretin induced significant calcium transients at the level previously defined as a "response" in seven out of eight of these spines. By contrast, only 2 out of the 26 control spines (in focus but not in apposition to a labeled bouton) responded to hypocretin, showing that spines that have appositions represent a significantly different population (Chi-square test: $\chi^2 = 20$; df = 1; $p < 0.0001$). It

Figure 2. Hypocretin Induces Glutamate Release Selectively onto a Subset of Spines on Apical Dendrites of Layer V Pyramidal Neurons

(A) Red, green, and ratio measurements from two spines on a short segment of apical dendrite: measurements from spines with red and blue arrows are shown by red diamonds and blue squares, respectively. Frames were acquired before (image 1), during (image 2), and after (not shown) the burst of spikes shown to the right. Note red intensity did not change during spikes, whereas spike-triggered calcium entry results in large increases in both green intensity and the green to red (G/R) ratio (seen in merged image as a shift from orange to yellow). Scale bar, 5 μm.

(B) Merged image shows another region of apical dendrite with multiple spines in focus. G/R ratio measurements for two example spines are shown in red and blue, respectively. Images of this portion of dendrite were acquired every 2 or 3 s during baseline (e.g., image 1), during hypocretin-induced sEPSCs (e.g., image 2), washout (not shown), and during a brief period of spiking triggered by depolarization (image 3). Inset shows region from yellow rectangle at higher magnification. Large, hypocretin-induced calcium transients (denoted by "*") were seen in the spine marked with the red arrow. Scale bars: regular, 5 μm; inset, 1 μm. Voltage-clamp sweeps illustrate electrophysiological activity, recorded at the soma, during the period in which the above frame was acquired.

(C) Graph showing that a group of spines (n = 7, red bars) showed peak G/R ratios during hypocretin which were similar or larger to those induced by spikes. By contrast, nearby spines in the same frames (n = 22, blue bars) behaved like the typical spine with little or no change from baseline during hypocretin application and large increase in G/R ratio seen only when spiking was induced (*$p < 0.001$, comparing mean Z peak during hypocretin in responders versus nonresponders).

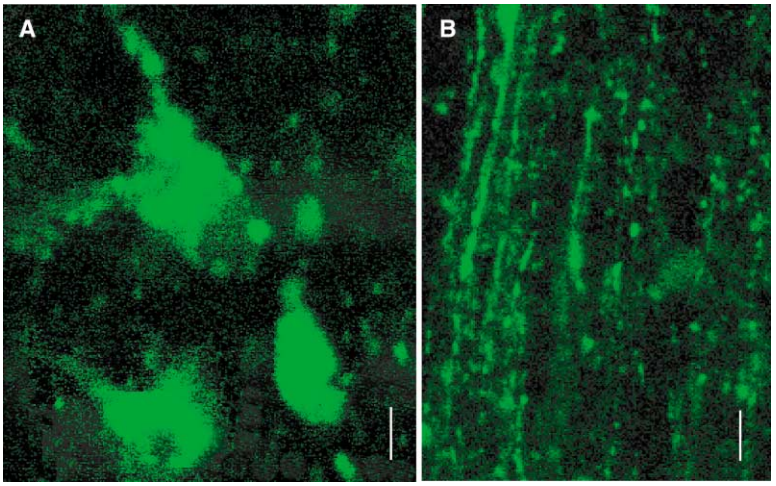

Figure 3. Thalamic Neurons and Axons Filled with the Anterograde Tracer *Phaseolus vulgaris* Conjugated to Alexa 488 Shown in Slices Taken 3 Days after In Vivo Bulk Electroporation

(A) Medial thalamic neurons labeled with PHAL488 in coronal slice taken at the level of the anterior thalamus. Scale bar, 10 μm.

(B) Thalamic axons coursing through white matter en route to frontal cortex, seen in horizontal slice at level of anterior cingulate. Scale bar, 8 μm.

was not unexpected to see a response in the occasional spine without an apparent apposition, since our electroporation protocol only labeled a portion of the neurons in the more anterior and dorsal nuclei of the thalamus. The graph in Figure 4C compares Z score means for spines in apposition (n = 8) and control spines from the same scans (n = 26). While virtually all spines with appositions showed significant G/R elevations during hypocretin, neither the mean G/R ratio (excluding peaks) for apposed spines nor their nonapposed controls increased significantly during hypocretin (nonapposed: basal, 0.39 ± 0.03; hypocretin, 0.40 ± 0.04; apposed: basal, 0.42 ± 0.04; hypocretin, 0.44 ± 0.04).

As an additional control group, we imaged six spines that were nearby (<3 μm) but not directly apposed to boutons or even a continuous axon, such as the one shown in the first part of Figure 5. None of these six spines showed a response to hypocretin. Even if the bouton was very close (1 μm in Figure 5B) but not touching in any Z section through the region, hypocretin-induced calcium transients were not observed. These data suggest that nonsynaptic volume transmission of glutamate is not sufficient to account for hypocretin-induced calcium transients.

Hypocretin-Induced Glutamate Release Is Blocked by Activation of μ-Opioid Receptors and Reduced Unilaterally by Prior Ipsilateral Thalamic Lesion

If, as hypothesized, hypocretin induces glutamate release through depolarization of thalamocortical boutons, it should be opposed physiologically by activation of the $G_{i/o}$-coupled μ-opioid receptors known to be present on those boutons (Marek et al., 2001). Figure 6A shows that selective μ-opioid receptor agonist DAMGO (1 μM; applied during and after hypocretin) almost completely suppressed hypocretin-induced sEPSCs (n = 5), as did the nonselective opioid agonist met-enkephalin (100 μM; applied during and after; n = 4; data not shown). DAMGO also suppressed calcium transients previously elicited by hypocretin at responding spines; this suppression was reversible (n = 2; data not shown).

To confirm the involvement of thalamic boutons, we made unilateral radiofrequency lesions in the thalamus and waited 2 weeks for degeneration of thalamocortical boutons. Baseline levels of sEPSCs did not differ significantly from those seen in normal animals, nor did they differ between the lesioned and the control hemispheres. As expected, hypocretin elicited a large increase in hypocretin-induced sEPSCs on the control, contralateral side (n = 6). By contrast, hypocretin-induced glutamate release onto layer V neurons was virtually eliminated in the cortex ipsilateral to the lesion, as illustrated in Figure 6B (n = 6).

Discussion

We have provided converging evidence that hypocretin excites thalamocortical boutons innervating spines on the apical dendrites of layer V neurons in anterior cingulate cortex. Almost without exception, spine heads receiving an apparent thalamocortical apposition responded to hypocretin with large, transient calcium increases congruent with multiple spiking events in their glutamatergic presynaptic afferents. These responses represent a lower limit on the magnitude and frequency of the events at these spines, due to the intermittent sampling technique employed. Since spines were imaged less than 3% of the time, each observed calcium transient could represent at least 30 nonimaged events at that spine. This imaging data was verified by electrophysiological and lesion data confirming the involvement of thalamocortical axons. Experiments in TTX showed no direct postsynaptic effect on layer V neurons of prefrontal cortex, which is consistent with the lack of hypocretin receptor 2 mRNA reported in these neurons (Marcus et al., 2001; Trivedi et al., 1998).

This represents the first demonstration of postsynaptic calcium transients resulting from neurotransmitter-elicited, TTX-sensitive depolarization of a population of axon terminals. Such observations are congruent with earlier studies suggesting that thalamocortical projections are prone to the generation of terminal spikes (Gutnick and Prince, 1972; Pinault and Pumain, 1989). Antidromic transmission of such spikes is thought to trigger bursting and strengthen synchronization of thalamic neurons (Pinault, 1995), especially those that project

densely into an overlapping cortical area. Single neuron tracing studies of the prefrontal axonal projections from midline and intralaminar thalamic neurons show that these neurons abundantly fulfill this criteria (Deschenes et al., 1996). These neurons exhibit unusual rapid rhythmic bursting in the awake animal (Steriade et al., 1993). The finding that hypocretin can excite the final synapse in the ascending arousal pathway, together with the unusual properties of thalamic terminals, suggests a mechanism for coordinating aspects of attention and arousal at a cortical level. Consistent with the idea of separate prefrontal modulation by hypocretin, recent work shows that prefrontal cortex receives projections from a distinct population of hypocretin neurons with minimal collaterals (Fadel et al., 2002).

Midline and Intralaminar Projections Appear to Target Spines on Branches of Apical Dendrites of Layer V Pyramidal Neurons

All responding spines were on branches of the apical dendrites, including many past the bifurcation and some in layer I. This localization is consistent with anatomical work showing that midline and intralaminar thalamic neurons afferents to cingulate cortex are dense in a superficial band and in another band in layer V (Berendse and Groenewegen, 1991). By documenting functional appositions, we build upon past ultrastructural studies of thalamic inputs to layer V pyramidal neurons in prefrontal cortex (Marini et al., 1996). It has been suggested that superficial inputs to layer V pyramidal neurons may be particularly influential in vivo since they are able to induce dendritic calcium action potentials which lead to bursts of sodium action potentials at the soma, particularly in "intrinsically bursting" layer V neurons of neocortex (Helmchen et al., 1999).

The neurons which receive these thalamocortical synapses excited by hypocretin are the major output neurons of prefrontal cortex; they project to almost every subcortical pathway that has been shown to be excited by hypocretin (Sutcliffe and de Lecea, 2002), including serotonergic, dopaminergic, cholinergic, and hypothalamic neurons (Groenewegen and Uylings, 2000). In this regard, the ability of hypocretin to excite thalamocortical synapses at key sites on layer V projection neurons may have broad physiological significance in that it completes a feedback circuit.

Effects of Hypocretin Are Strongly Opposed by μ-Opioid Stimulation

The ability of hypocretin to induce glutamate release from thalamocortical boutons can be suppressed by activation of μ-opioid receptors. Physiological antagonism between μ-opioids and hypocretin in the thalamocortical pathway has not previously been suspected. Previous work has localized μ-opioid receptors to thalamocortical boutons (Marek et al., 2001) and showed that μ-opioid agonists do not block cortico-cortical excitatory transmission (Tanaka and North, 1994). The opposite effects of hypocretin (Sutcliffe and de Lecea, 2002) and opiates (Giacchino and Henriksen, 1998) on arousal and alertness may be based on their opposing actions at thalamic boutons as well as their actions at thalamic cell bodies, although the latter has not been tested. The ability of enkephalin to suppress hypocretin-induced sEPSCs further suggests the possibility that enkephalin-containing interneurons (McGinty et al., 1984) may be able to circumvent hypocretin stimulation of thalamocortical boutons in the cortex. Anterior cingulate is known to be a supraspinal target for both endogenous and exogenous opioids (Giacchino and Henriksen, 1998; Tanaka and North, 1994; Zubieta et al., 2001).

Implications for Cortical Arousal and Attention

Hypocretin levels have been shown to correlate with states of attention and arousal (Sutcliffe and de Lecea, 2002), with high levels observed during alertness and periods of physical activity (Kiyashchenko et al., 2002; Wu et al., 2002; Yoshida et al., 2001). Using a novel approach that combined the labeling of presynaptic thalamocortical boutons with calcium imaging in postsynaptic spines of layer V cortical pyramidal neurons, we have provided evidence for selective activation of thalamocortical boutons in prefrontal cortex by hypocretin. This is the first use of two-photon imaging in dendritic spines to examine calcium transients elicited by neurotransmitter acting upon excitatory presynaptic receptors. In addition to triggering glutamate-mediated postsynaptic excitation, the ability of hypocretin released in prefrontal cortex to trigger antidromic spikes in these multiple-branched thalamocortical projections would tend to coordinate the bursting of midline and intralaminar thalamic neurons in vivo. We have demonstrated that hypocretin in prefrontal cortex can activate a mechanism in vitro which has the potential to affect alertness and attention in vivo. These results raise questions about the regulation of hypocretin release within prefrontal cortex in healthy subjects. The answers may clarify why patients with narcolepsy show specific impairment in the executive attention network (Rieger et al., 2003) and abnormal frontal physiology during preattentive and attentive tasks (Naumann et al., 2001).

Experimental Procedures

Whole-Cell Recordings in Pyramidal Neurons

Coronal prefrontal slices (400–500 μm thick) were prepared from Sprague-Dawley rats 20–50 days old, in accordance with protocols approved by the Yale University Animal Care and Use committee. Slices were cut in chilled, oxygenated ACSF in which 252 mM sucrose was substituted for NaCl, then placed in a modified chamber (Warner Instruments, Hamden, CT) under a modified slice hold-down device (Warner Instruments). Regular ACSF (126 mM NaCl, 3 mM KCl, 1.25 mM NaH_2PO_4, 10 mM D-glucose, 25 mM $NaHCO_3$, 2 mM $CaCl_2$, and 2 mM $MgSO_4$ [pH 7.35]) was bubbled with 95% oxygen-5% carbon dioxide, warmed, and flowed over slice at 30°C (4 ml/minute). Whole-cell patch electrodes (4–6 MΩ) contained 115 mM potassium gluconate, 20 mM KCl, 2 mM Mg-ATP, 1 mM Na_2-ATP, 10 mM Na_2-phosphocreatine, 0.3 mM Tris-GTP, and 10 mM HEPES (pH 7.33). For calcium imaging, patch solution included 100–200 μM Oregon green BAPTA-1 and 10–20 μM Alexa 594 hydrazide (Molecular Probes, Eugene, OR). Neurons were patched under visual control with IR-DIC, and access resistance was maintained at $<$12 MΩ.

Synaptic currents and direct postsynaptic effects were recorded using continuous single electrode voltage-clamp mode with an Axoclamp 2A (Axon Instruments, Union City, CA). Spontaneously occurring excitatory postsynaptic currents (sEPSCs) were low-pass filtered at 3 kHz, amplified 100× through Cyberamp and digitized at 15 kHz, and acquired using pClamp/Digidata 1200 (Axon Instru-

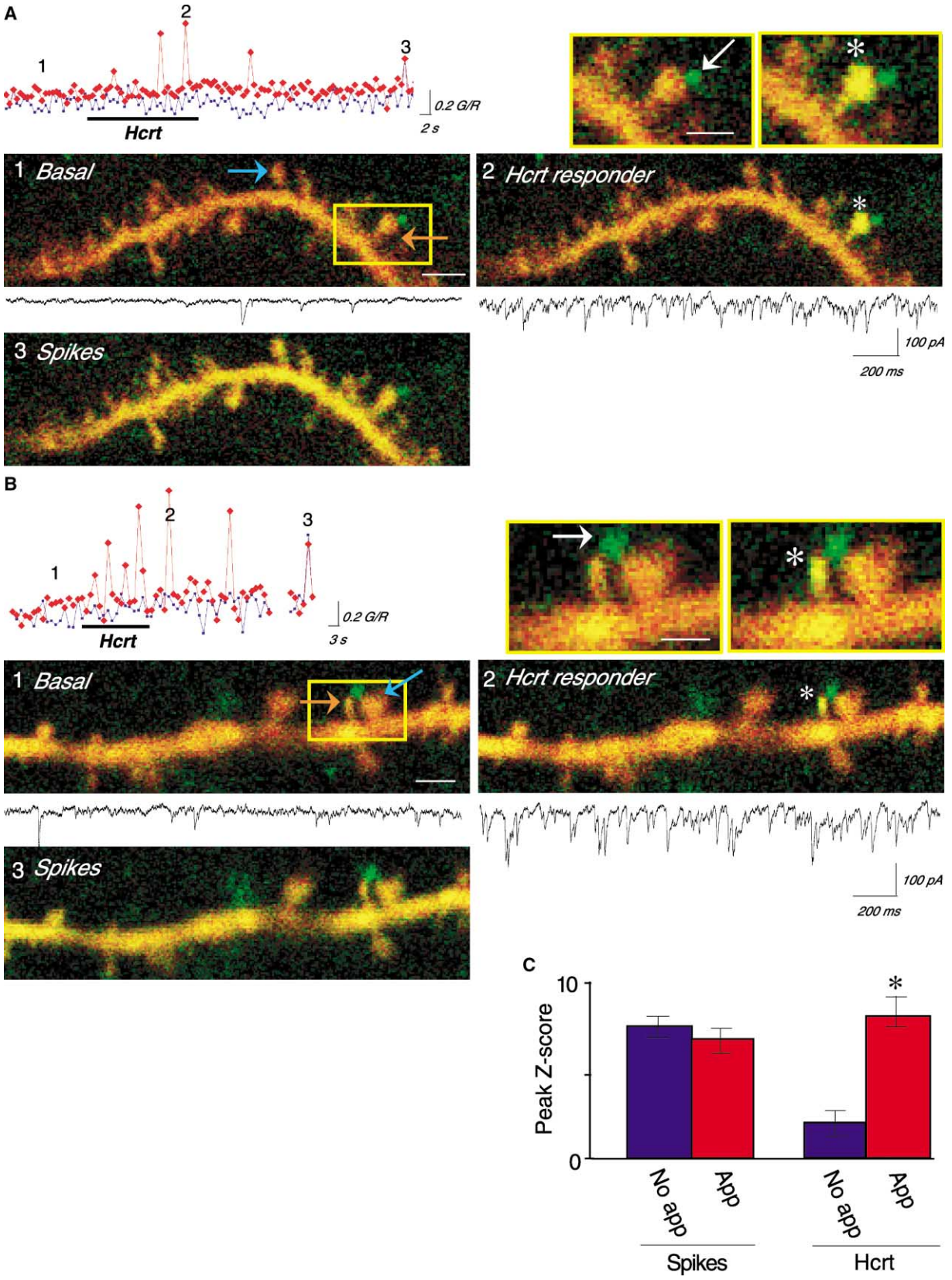

Figure 4. Spines in Apposition to Identified Thalamocortical Boutons Showed Calcium Transients in Response to Hypocretin

(A) G/R ratio measurements for two spines on a branch of apical dendrite: the red arrow points to spine in apparent apposition to a labeled bouton (white arrow) and the blue arrow to a nearby spine in focus. In the merged image, the orange dendrites and spines can be readily

ments). Analysis of sEPSCs from each 10 s block of (1 s) sweeps was performed using MiniAnalysis software (Synaptosoft Inc., Decatur, GA). This program detects and measures spontaneous synaptic events according to amplitude, rise time, decay time, and area under the curve. As a result of the high frequency of sEPSCs, the ability to measure overlapping or closely occurring peaks accurately is important for our analysis. The software uses an algorithm to detect multiple and complex peaks and automatically adjusts the baseline of closely occurring peaks using exponential extrapolation of decay. Amplitude and area thresholds were set to 8 pA and 25–50 fC, respectively. Given our noise level of ~5 pA, this combination of thresholds maximized correct identification of sEPSCs and minimized false positives. Changes in frequency and amplitude of spontaneous excitatory postsynaptic currents (sEPSC) within individual neurons were assessed by Kolmogorov-Smirnov tests of distribution on binned data from 20 (1 s) sweeps in voltage clamp during hypocretin compared to baseline. Group statistical significance was assessed using paired Student's t tests. Unless stated otherwise, averages are expressed as mean ± standard error of the mean (SEM).

For preliminary electrophysiology, neurons were held near resting potential at −70 mV. For calcium imaging, bath solution was changed to 0.5 mM $MgSO_4$ and 3 mM $CaCl_2$, and neurons were held at −60 mV to increase calcium entry through NMDA receptors. Hypocretin-2 peptide, in ACSF, was applied for 1 min at a time in the fast-flowing bath, followed by a washout period of 10–45 min. Hypocretin-2 peptide was a gift from Dr. Anthony Van den Pol (Yale University) and LY293558 was a gift from Eli Lilly (Indianapolis, IN). Orexin B (hypocretin-1 peptide) was from Phoenix Pharmaceuticals (Belmont, CA). Unless otherwise specified, all drugs were from Sigma-Aldrich (St. Louis, MO).

Bulk Electroporation to Label Thalamic Projections

Two to five days prior to cutting slices and recording, a subgroup of animals received surgery to bulk electroporate (Haas et al., 2001, 2002; Saito and Nakatsuji, 2001) neurons of the anterior and dorsal left thalamus with the anterograde tracer *Phaseolus vulgaris* conjugated with Alexa 488 (PHAL488, 10 μg/μL, Molecular Probes). Surgery was performed using the method described previously (Lambe and Aghajanian, 2001; Lambe et al., 2003). In brief, after anesthesia with sterile choral hydrate (400 mg/kg), a Hamilton syringe, with a needle insulated except for the tip, was lowered through a burr hole to the following coordinates in relation to Bregma: 0.75 mm lateral, 2.5 mm posterior, 5.5 mm deep. The anterograde tracer was injected 0.5 μl per time at intervals of 5 min to a total of 2 μl, and the syringe was lifted 0.25 μm before the next injection. Electroporation was achieved with the following current parameters applied over the entire time of injection (25 min): 500 ms train consisting of 12 stimuli of 35 μA alternating with 500 ms of no current pulses.

Two-Photon Calcium Imaging and Analysis

We used a two-photon laser scanning system consisting of a Ti:sapphire laser (Mai Tai, Spectra Physics, Mountain View, CA) tuned to wavelength 810 nm and a direct detection Bio-Rad Radiance 2100 MP (Bio-Rad Microscience, Hemel Hempstead, UK) on an Olympus BX50WI microscope (Olympus, Melville, NY) with an ×60, 0.9 NA water-immersion objective (Olympus). Green and red emitted fluorescence were separated with a dichroic DC560LP (Olympus) and filtered with HG515/30 and HQ620/100 filters (Olympus), respectively.

Layer V pyramidal neurons were filled through the patch pipette with the high-affinity (K_d 170 nM) Oregon Green BAPTA-1, in order to maximize the possibility of detecting sporadic calcium transients with our sampling parameters (described below). The calcium indicator was combined with a red fluorophore, Alexa 594 hydrazide, to facilitate visualization of spines and allow ratio measurements of total green to total red intensity (G/R), which compensate for small movements (Oertner et al., 2002). Pipettes were tip filled with regular patch solution to avoid ejecting dye from the pipette into the extracellular space of the slice; cells with detectable background fluorescence after dye loading were not used. Subtraction of photodetector dark current was the only background correction performed.

Since the pharmacological manipulations of interest did not allow control over the timing of synaptic events at any spine, regions of dendrite were sampled every 2 to 3 s during baseline (45 s), bath application of hypocretin (1 min), and washout (2–3 min), as well as during depolarization-induced spikes. Imaging frames were 512 pixels by 200 lines (4–6× zoom, 750 lps). This sampling protocol was chosen to reduce the chance of photobleaching and phototoxicity to spines. In order to enhance detection of calcium transients, which are largely mediated by NMDA receptors (Kovalchuk et al., 2000; Mainen et al., 1999; Oertner et al., 2002; Yuste and Denk, 1995), we voltage clamped the layer V pyramidal neurons at −60 mV in 0.25–0.5 mM Mg^{2+}, 3mM Ca^{2+} ACSF. Spontaneous EPSCs were measured continuously during scanning. Since the sampling protocol meant that we were unlikely to catch transients at their peak, the indicator and concentration used were selected to achieve a balance between amplitude and duration of transient. For experiments on slices from animals with labeled thalamocortical projections, we included only apparent appositions between bouton and spine in the *x-y* plane to maximize resolution and reduce possibility of movement-related artifacts.

Images were analyzed with c-Imaging software (Compix Imaging, Cranberry Township, PA). For each region of dendrite, the series of images was analyzed by drawing regions of interest (ROIs) on spine heads in focus and measuring total red and total green intensities for each ROI from each frame in the series. Scan series were not included in the final analysis if movement or photobleaching (observed as a progressive decline in the red total intensity measurement) had occurred. Green to red (G/R) ratio measurements from baseline period were averaged to calculate Z scores for each image taken during and following hypocretin application, as well as during depolarization-induced spikes. The peak Z score measurement was used to compare for each spine peak G/R increase during hypocretin with that observed during spikes.

Unilateral Thalamic Lesions

Two weeks prior to cutting slices and recording, a subgroup of animals received radiofrequency lesions to the anterior-dorsal left thalamus. Surgery was performed as described above. An insulated #1 insect pin was lowered through a burr hole to the same coordinates as above. A radiofrequency current (20 mA, 1000 kHz) was passed for 1 min. The pin was removed and the incision sutured. All animals recovered quickly and were in good health during the 2 week, postlesion period allowed for degeneration of thalamocortical boutons. For recording, slices were positioned to allow access to the medial prefrontal cortex on both hemispheres. Neurons from prefrontal cortex contralateral to the lesion were used as controls. The thalamus was also sectioned to verify the position of the lesion.

distinguished from the green-labeled boutons. Images of this region were taken every 2 s. Example frames are included from baseline (image 1) and during application of hypocretin (image 2); inset shows magnification of area from yellow rectangle. Note large calcium transient (*) during hypocretin application in spine apposed to thalamic bouton but no change in nearby spines without apposition. Scale bars: regular, 5 μm; inset, 2 μm. Sweeps in voltage clamp show electrophysiological activity, measured at the soma, surrounding the time of above frame acquisition.

(B) An additional example shows two spines in apparent apposition to a single labeled bouton. Only the spine to the left (with the red arrow) showed large calcium transients during application of hypocretin. Scale bars: regular, 4 μm; inset, 2 μm.

(C) Graph shows mean ± SEM peak change in G/R ratio from baseline during spikes and hypocretin for spines apposed to thalamocortical boutons (n = 8, red bars) versus nearby spines in focus but not in apparent apposition to a green bouton (n = 26, blue bars). *$p < 0.001$, comparing mean hypocretin peak in spines in apparent apposition to a thalamic bouton versus other spines in focus in the same field.

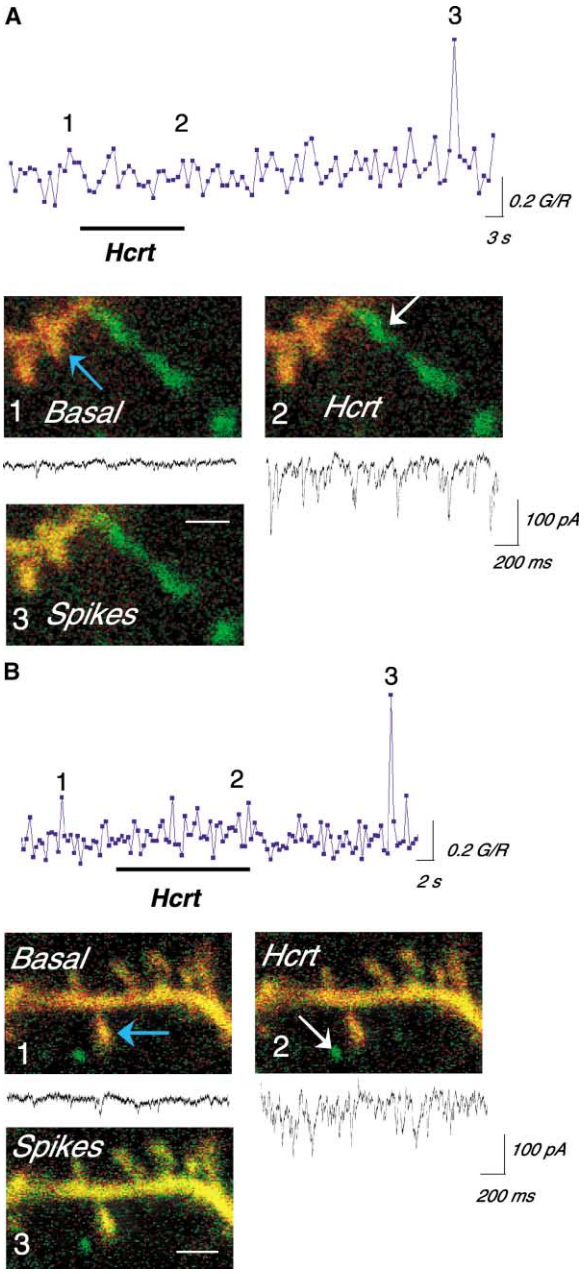

Figure 5. Control Spines which Were Close to but Not "Touching" Identified Thalamocortical Boutons Did Not Show Large Calcium Transients in Response to Hypocretin

(A) A control example shows a thalamocortical axon passing nearby but not in apposition to a spine. This spine showed little or no change in G/R ratios during hypocretin-induced sEPSCs; however, as shown below, G/R increased dramatically with depolarization-induced spikes. Scale bar, 2 μm.

(B) Even a bouton which was very close (1 μm, but not touching in any Z section) was not associated with calcium transients in the nearby spine. Scale bar, 2 μm.

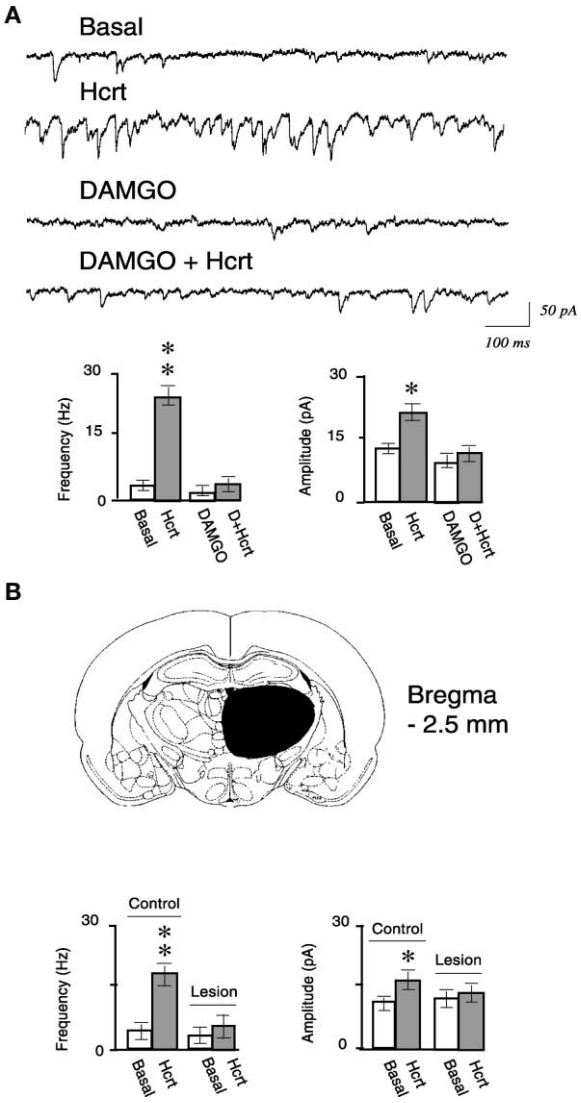

Figure 6. The Selective μ-Opioid Agonist DAMGO Opposes Hypocretin-Induced Glutamate Release, and Prior Unilateral Thalamic Lesion Reduces Hypocretin-Induced sEPSCs Ipsilaterally

(A) DAMGO (1 μM, 2 min) almost completely suppressed hypocretin-induced sEPSCs, presumably through a physiological antagonism ($n = 5$ neurons; hypocretin, 100 nM for 1 min; $^{**}p < 0.001$; $^{*}p < 0.01$).

(B) Unilateral radiofrequency lesion to the thalamus resulted in an ipsilateral loss of hypocretin-induced sEPSCs in prefrontal cortex ($n = 6$). Significant hypocretin-induced increases in sEPSC frequency and amplitude were still observed in prefrontal cortex of the control hemisphere ($n = 6$ neurons; hypocretin, 100 nM for 1 min; $^{**}p < 0.01$; $^{*}p < 0.05$). Basal sEPSC frequency and amplitude in both hemispheres of lesioned animals were within the range observed in nonlesioned animals.

Received: June 3, 2003
Revised: August 20, 2003
Accepted: September 5, 2003
Published: September 24, 2003

Acknowledgments

We thank Dr. Meenakshi Alreja and Dr. Mark Yeckel for valuable discussions and comments on the manuscript. This project was supported by NIH grant MH17871.

References

Bayer, L., Eggermann, E., Saint-Mleux, B., Machard, D., Jones, B.E., Muhlethaler, M., and Serafin, M. (2002). Selective action of orexin

(hypocretin) on nonspecific thalamocortical projection neurons. J. Neurosci. *22*, 7835–7839.

Berendse, H.W., and Groenewegen, H.J. (1991). Restricted cortical termination fields of the midline and intralaminar thalamic nuclei in the rat. Neuroscience *42*, 73–102.

Chemelli, R.M., Willie, J.T., Sinton, C.M., Elmquist, J.K., Scammell, T., Lee, C., Richardson, J.A., Williams, S.C., Xiong, Y., Kisanuki, Y., et al. (1999). Narcolepsy in orexin knockout mice: molecular genetics of sleep regulation. Cell *98*, 437–451.

Deschenes, M., Bourassa, J., and Parent, A. (1996). Striatal and cortical projections of single neurons from the central lateral thalamic nucleus in the rat. Neuroscience *72*, 679–687.

Fadel, J., and Deutch, A.Y. (2002). Anatomical substrates of orexin-dopamine interactions: lateral hypothalamic projections to the ventral tegmental area. Neuroscience *111*, 379–387.

Fadel, J., Bubser, M., and Deutch, A.Y. (2002). Differential activation of orexin neurons by antipsychotic drugs associated with weight gain. J. Neurosci. *22*, 6742–6746.

Giacchino, J.L., and Henriksen, S.J. (1998). Opioid effects on activation of neurons in the medial prefrontal cortex. Prog. Neuropsychopharmacol. Biol. Psychiatry *22*, 1157–1178.

Groenewegen, H.J., and Berendse, H.W. (1994). The specificity of the 'nonspecific' midline and intralaminar thalamic nuclei. Trends Neurosci. *17*, 52–57.

Groenewegen, H.J., and Uylings, H.B. (2000). The prefrontal cortex and the integration of sensory, limbic and autonomic information. Prog. Brain Res. *126*, 3–28.

Gutnick, M.J., and Prince, D.A. (1972). Thalamocortical relay neurons: antidromic invasion of spikes from a cortical epileptogenic focus. Science *176*, 424–426.

Haas, K., Sin, W.C., Javaherian, A., Li, Z., and Cline, H.T. (2001). Single-cell electroporation for gene transfer in vivo. Neuron *29*, 583–591.

Haas, K., Jensen, K., Sin, W.C., Foa, L., and Cline, H.T. (2002). Targeted electroporation in Xenopus tadpoles in vivo–from single cells to the entire brain. Differentiation *70*, 148–154.

Helmchen, F., Svoboda, K., Denk, W., and Tank, D.W. (1999). In vivo dendritic calcium dynamics in deep-layer cortical pyramidal neurons. Nat. Neurosci. *2*, 989–996.

Hofle, N., Paus, T., Reutens, D., Fiset, P., Gotman, J., Evans, A.C., and Jones, B.E. (1997). Regional cerebral blood flow changes as a function of delta and spindle activity during slow wave sleep in humans. J. Neurosci. *17*, 4800–4808.

Jones, E.G. (2001). The thalamic matrix and thalamocortical synchrony. Trends Neurosci. *24*, 595–601.

Kiyashchenko, L.I., Mileykovskiy, B.Y., Maidment, N., Lam, H.A., Wu, M.F., John, J., Peever, J., and Siegel, J.M. (2002). Release of hypocretin (orexin) during waking and sleep states. J. Neurosci. *22*, 5282–5286.

Kovalchuk, Y., Eilers, J., Lisman, J., and Konnerth, A. (2000). NMDA receptor-mediated subthreshold Ca (2+) signals in spines of hippocampal neurons. J. Neurosci. *20*, 1791–1799.

Lambe, E.K., and Aghajanian, G.K. (2001). The role of Kv1.2-containing potassium channels in serotonin-induced glutamate release from thalamocortical terminals in rat frontal cortex. J. Neurosci. *21*, 9955–9963.

Lambe, E.K., Picciotto, M.R., and Aghajanian, G.K. (2003). Nicotine induces glutamate release from thalamocortical terminals in prefrontal cortex. Neuropsychopharmacology *28*, 216–225.

Lin, L., Faraco, J., Li, R., Kadotani, H., Rogers, W., Lin, X., Qiu, X., de Jong, P.J., Nishino, S., and Mignot, E. (1999). The sleep disorder canine narcolepsy is caused by a mutation in the hypocretin (orexin) receptor 2 gene. Cell *98*, 365–376.

Mainen, Z.F., Malinow, R., and Svoboda, K. (1999). Synaptic calcium transients in single spines indicate that NMDA receptors are not saturated. Nature *399*, 151–155.

Marcus, J.N., Aschkenasi, C.J., Lee, C.E., Chemelli, R.M., Saper, C.B., Yanagisawa, M., and Elmquist, J.K. (2001). Differential expression of orexin receptors 1 and 2 in the rat brain. J. Comp. Neurol. *435*, 6–25.

Marek, G.J., Wright, R.A., Gewirtz, J.C., and Schoepp, D.D. (2001). A major role for thalamocortical afferents in serotonergic hallucinogen receptor function in the rat neocortex. Neuroscience *105*, 379–392.

Marini, G., Pianca, L., and Tredici, G. (1996). Thalamocortical projection from the parafascicular nucleus to layer V pyramidal cells in frontal and cingulate areas of the rat. Neurosci. Lett. *203*, 81–84.

McCormick, D.A., and Bal, T. (1997). Sleep and arousal: thalamocortical mechanisms. Annu. Rev. Neurosci. *20*, 185–215.

McCormick, D.A., and Contreras, D. (2001). On the cellular and network bases of epileptic seizures. Annu. Rev. Physiol. *63*, 815–846.

McGinty, J.F., van der Kooy, D., and Bloom, F.E. (1984). The distribution and morphology of opioid peptide immunoreactive neurons in the cerebral cortex of rats. J. Neurosci. *4*, 1104–1117.

Naumann, A., Bierbrauer, J., Przuntek, H., and Daum, I. (2001). Attentive and preattentive processing in narcolepsy as revealed by event-related potentials (ERPs). Neuroreport *12*, 2807–2811.

Oertner, T.G., Sabatini, B.L., Nimchinsky, E.A., and Svoboda, K. (2002). Facilitation at single synapses probed with optical quantal analysis. Nat. Neurosci. *5*, 657–664.

Paus, T., Koski, L., Caramanos, Z., and Westbury, C. (1998). Regional differences in the effects of task difficulty and motor output on blood flow response in the human anterior cingulate cortex: a review of 107 PET activation studies. Neuroreport *9*, R37–R47.

Peyron, C., Tighe, D.K., van den Pol, A.N., de Lecea, L., Heller, H.C., Sutcliffe, J.G., and Kilduff, T.S. (1998). Neurons containing hypocretin (orexin) project to multiple neuronal systems. J. Neurosci. *18*, 9996–10015.

Peyron, C., Faraco, J., Rogers, W., Ripley, B., Overeem, S., Charnay, Y., Nevsimalova, S., Aldrich, M., Reynolds, D., Albin, R., et al. (2000). A mutation in a case of early onset narcolepsy and a generalized absence of hypocretin peptides in human narcoleptic brains. Nat. Med. *6*, 991–997.

Pinault, D. (1995). Backpropagation of action potentials generated at ectopic axonal loci: hypothesis that axon terminals integrate local environmental signals. Brain Res. Brain Res. Rev. *21*, 42–92.

Pinault, D., and Pumain, R. (1989). Antidromic firing occurs spontaneously on thalamic relay neurons: triggering of somatic intrinsic burst discharges by ectopic action potentials. Neuroscience *31*, 625–637.

Rieger, M., Mayer, G., and Gauggel, S. (2003). Attention deficits in patients with narcolepsy. Sleep *26*, 36–43.

Ripley, B., Overeem, S., Fujiki, N., Nevsimalova, S., Uchino, M., Yesavage, J., Di Monte, D., Dohi, K., Melberg, A., Lammers, G.J., et al. (2001). CSF hypocretin/orexin levels in narcolepsy and other neurological conditions. Neurology *57*, 2253–2258.

Saito, T., and Nakatsuji, N. (2001). Efficient gene transfer into the embryonic mouse brain using in vivo electroporation. Dev. Biol. *240*, 237–246.

Sakurai, T., Amemiya, A., Ishii, M., Matsuzaki, I., Chemelli, R.M., Tanaka, H., Williams, S.C., Richardson, J.A., Kozlowski, G.P., Wilson, S., et al. (1998). Orexins and orexin receptors: a family of hypothalamic neuropeptides and G protein-coupled receptors that regulate feeding behavior. Cell *92*, 573–585.

Steriade, M., Curro Dossi, R., and Contreras, D. (1993). Electrophysiological properties of intralaminar thalamocortical cells discharging rhythmic (approximately 40 HZ) spike-bursts at approximately 1000 HZ during waking and rapid eye movement sleep. Neuroscience *56*, 1–9.

Sutcliffe, J.G., and de Lecea, L. (2002). The hypocretins: setting the arousal threshold. Nat. Rev. Neurosci. *3*, 339–349.

Tanaka, E., and North, R.A. (1994). Opioid actions on rat anterior cingulate cortex neurons in vitro. J. Neurosci. *14*, 1106–1113.

Thannickal, T.C., Moore, R.Y., Nienhuis, R., Ramanathan, L., Gulyani, S., Aldrich, M., Cornford, M., and Siegel, J.M. (2000). Reduced number of hypocretin neurons in human narcolepsy. Neuron *27*, 469–474.

Trivedi, P., Yu, H., MacNeil, D.J., Van der Ploeg, L.H., and Guan,

X.M. (1998). Distribution of orexin receptor mRNA in the rat brain. FEBS Lett. *438*, 71–75.

Wu, M.F., John, J., Maidment, N., Lam, H.A., and Siegel, J.M. (2002). Hypocretin release in normal and narcoleptic dogs after food and sleep deprivation, eating, and movement. Am. J. Physiol. Regul. Integr. Comp. Physiol. *283*, R1079–R1086.

Yamasaki, H., LaBar, K.S., and McCarthy, G. (2002). Dissociable prefrontal brain systems for attention and emotion. Proc. Natl. Acad. Sci. USA *99*, 11447–11451.

Yoshida, Y., Fujiki, N., Nakajima, T., Ripley, B., Matsumura, H., Yoneda, H., Mignot, E., and Nishino, S. (2001). Fluctuation of extracellular hypocretin-1 (orexin A) levels in the rat in relation to the light-dark cycle and sleep-wake activities. Eur. J. Neurosci. *14*, 1075–1081.

Yuste, R., and Denk, W. (1995). Dendritic spines as basic functional units of neuronal integration. Nature *375*, 682–684.

Zubieta, J.K., Smith, Y.R., Bueller, J.A., Xu, Y., Kilbourn, M.R., Jewett, D.M., Meyer, C.R., Koeppe, R.A., and Stohler, C.S. (2001). Regional mu opioid receptor regulation of sensory and affective dimensions of pain. Science *293*, 311–315.